Cytotherapy 000 (2020) 1–13

Contents lists available at ScienceDirect

CYTOTHERAPY

journal homepage: www.isct-cytotherapy.org

# Regulatory-compliant conditions during cell product manufacturing enhance *in vitro* immunomodulatory properties of infrapatellar fat pad-derived mesenchymal stem/stromal cells

Dimitrios Kouroupis[1,2], Annie C. Bowles[1,2,3], Dylan N. Greif[1], Clarissa Leñero[1,2,4], Thomas M. Best[1], Lee D. Kaplan[1], Diego Correa[1,2,*]

[1] *Department of Orthopedics, UHealth Sports Medicine Institute, University of Miami Miller School of Medicine, Miami, Florida, USA*
[2] *Diabetes Research Institute & Cell Transplant Center, University of Miami Miller School of Medicine, Miami, Florida, USA*
[3] *Department of Biomedical Engineering, University of Miami College of Engineering, Miami, Florida, USA*
[4] *Cryovida Banco de Células Madre Adultas, Guadalajara, Jalisco, Mexico*

ARTICLE INFO

*Article History:*
Received 5 March 2020
Accepted 25 June 2020
Available online xxx

*Key Words:*
cell product manufacturing
cell therapy
human platelet lysate
immunomodulation
infrapatellar fat pad
mesenchymal stem/stromal cells

ABSTRACT

*Background aims:* Mesenchymal stem/stromal cell (MSC)-based therapies have gained attention as potential alternatives for multiple musculoskeletal indications based on their trophic and immunomodulatory properties. The infrapatellar fat pad (IFP) serves as a reservoir of MSCs, which play crucial roles modulating inflammatory and fibrotic events at the IFP and its neighboring tissue, the synovium. In an effort to comply with the existing regulatory framework regarding cell-based product manufacturing, we interrogated the *in vitro* immunomodulatory capacity of human-derived IFP-MSCs processed under different conditions, including a regulatory-compliant protocol, in addition to their response to the inflammatory and fibrotic environments often present in joint disease.

*Methods:* Immunophenotype, telomere length, transcriptional and secretory immunomodulatory profiles and functional immunopotency assay were assessed in IFP-MSCs expanded in regular fetal bovine serum (FBS)-supplemented medium and side-by-side compared with same-donor cells processed with two media alternatives (i.e., regulatory-compliant pooled human platelet lysate [hPL] and a chemically reinforced/serum-reduced [Ch-R] formulation). Finally, to assess the effects of such formulations on the ability of the cells to respond to pro-inflammatory and pro-fibrotic conditions, all three groups were stimulated *ex vivo* (i.e., cell priming) with a cocktail containing TNF$\alpha$, IFN$\gamma$ and connective tissue growth factor (tumor-initiating cells) and compared with non-induced cohorts assessing the same outcomes.

*Results:* Non-induced and primed IFP-MSCs expanded in either hPL or Ch-R showed distinct morphology *in vitro*, similar telomere dynamics and distinct phenotypical and molecular profiles when compared with cohorts grown in FBS. Gene expression of IL-8, CD10 and granulocyte colony-stimulating factor was highly enriched in similarly processed IFP-MSCs. Cell surface markers related to the immunomodulatory capacity, including CD146 and CD10, were highly expressed, and secretion of immunomodulatory and pro-angiogenic factors was significantly enhanced with both hPL and Ch-R formulations. Upon priming, the immunomodulatory phenotype was enhanced, resulting in further increase in CD146 and CD10, significant CXCR4 presence and reduction in TLR3. Similarly, transcriptional and secretory profiles were enriched and more pronounced in IFP-MSCs expanded in either hPL or Ch-R, suggesting a synergistic effect between these formulations and inflammatory/fibrotic priming conditions. Collectively, increased indoleamine-2,3-dioxygenase activity and prostaglandin E2 secretion for hPL- and Ch-R-expanded IFP-MSCs were functionally reflected by their robust T-cell proliferation suppression capacity *in vitro* compared with IFP-MSCs expanded in FBS, even after priming.

*Conclusions:* Compared with processing using an FBS-supplemented medium, processing IFP-MSCs with either hPL or Ch-R similarly enhances their immunomodulatory properties, which are further increased after exposure to an inflammatory/fibrotic priming environment. This evidence supports the adoption of regulatory-compliant practices during the manufacturing of a cell-based product based on IFP-MSCs and anticipates a further enhanced response once the cells face the pathological environment after

* Correspondence: Diego Correa, MD, MSc, PhD, Diabetes Research Institute & Cell Transplant Center, University of Miami Miller School of Medicine, 1450 NW 10th Ave, Rm 3014, Miami, Florida 33136, USA.
*E-mail address:* dxc821@med.miami.edu (D. Correa).

https://doi.org/10.1016/j.jcyt.2020.06.007

intra-articular administration. Mechanistically, the resulting functionally enhanced cell-based product has potential utilization as a novel, minimally invasive cell therapy for joint disease through modulation of local immune and inflammatory events.



## Introduction

The infrapatellar fat pad (IFP) is an intracapsular/extrasynovial tissue with reported biomechanical functions inside the knee [1,2] and has recently gained attention as a key player in joint homeostasis. The IFP and the neighboring synovium constitute a functional anatomical unit [3], playing crucial roles in the establishment and progression of joint disease, including osteoarthritis (OA), where inflammatory and fibrotic microenvironments are present [4–8]. Mesenchymal stem/stromal cells (MSCs) possess immunomodulatory and trophic effects involving anti-inflammatory, angiogenic and antifibrotic activities [9]. The IFP constitutes a promising alternative source of MSCs [10–14] given the ease of harvest during knee arthroscopy [15], relative higher cell yield compared with bone marrow, higher expansive and *in vitro* differentiation profiles of IFP-MSC compared with other MSC types [16,17] and the fact that they naturally reside within the joint environment. We have previously reported that IFP-MSCs expanded in "regular" fetal bovine serum (FBS)-containing media control key local pathological mediators, including Substance P degradation, both *in vitro* and *in vivo*, while suppressing the proliferation of peripheral blood mononuclear cells (PBMCs) in a dose-dependent manner [18]. These effects are enhanced with prior *ex vivo* exposure of the cells (i.e., cell priming) to TNF$\alpha$/IFN$\gamma$/connective tissue growth factor (tumor-initiating cells [TICs]), a cocktail that molecularly mimics a synovitis and IFP fibrosis environment, inducing IFP-MSCs to be effectively suppressive of PBMCs, even at significantly reduced numbers [18].

To date, FBS supplementation of MSC growth media constitutes the standard of care worldwide, with almost 80% of clinical trials using MSCs exposed to animal derivatives. However, numerous studies have raised safety concerns regarding the use of FBS-containing media during MSC manufacturing for clinical applications [19–21]. Furthermore, large-scale manufacturing under such conditions may result in modifications to various cell characteristics and attributes, including phenotypic and functional alterations. In addition to inherent donor variability, these alterations may negatively affect the standardization and reproducibility of therapeutic outcomes, which may explain the variable efficacy seen in various clinical trials. In light of these issues, various studies have highlighted the importance of MSC "fitness" [22,23] in yielding improved MSC functionalities for better therapeutics *in vivo*.

In response to the growing need to replace FBS during MSC-based product manufacturing for regenerative medicine purposes, especially in large-scale manufacturing, the use of human platelet derivatives such as platelet lysate has been proposed. In a pioneering study, Doucet *et al.* [24] proposed human platelet lysate (hPL) as a potent source of bioactive molecules stored in platelets' $\alpha$-granules for the *ex vivo* expansion of MSCs. Among the bioactive molecules are those within the families of mitogenic growth factors, including platelet-derived growth factor (PDGF), epidermal growth factor (EGF), insulinlike growth factor, transforming growth factor (TGF) and fibroblast growth factor 2 [25,26]. Different positive outcomes have been assessed in MSCs obtained from various sources and processed with hPL when compared with expansion with FBS, including proliferation as colony-forming unit fibroblasts, differentiation potential, senescence, chromosomal stability and angiogenesis [27–35]. Furthermore, pilot clinical trials investigating the immunosuppressive effects of MSCs expanded in hPL to treat acute and chronic graft-versus-host disease observed no early or late adverse effects at a median follow-up of 8 months, including patients receiving up to five cell infusions [36,37]. More importantly, in a recent survey by Phinney and Galipeau [38] aimed at defining Good Manufacturing Practices in US academic centers, it was found that most centers expand MSCs in media supplemented with pooled hPL. Notwithstanding this evidence, the authors also mentioned that the effects of hPL on MSCs are still subject to scrutiny given contrasting results reported in the literature. For instance, some groups have reported differences in differentiation and immunomodulatory potentials in bone marrow- and adipose-derived MSCs processed in either hPL or FBS [39], while others have not [30,40]. Therefore, the authors suggest that resolving these discrepancies becomes paramount during the manufacturing of cell-based products that have consistent potencies and are intended for specific clinical indications. In parallel, efforts have recently been made to develop synthetic serum-reduced and serum-free replacements for MSC manufacturing [41,42]. These synthetic media contain a mixture of recombinant bioactive molecules, such as proteins, hormones, cytokines and/or growth factors, that supplement the culture media, "compensating" for the reduction or lack of serum. Here we use an optimized low-serum formulation (2% FBS) supplemented with a cocktail of defined compounds (final composition undisclosed because of the manufacturer's proprietary restrictions) that falls into that category, corresponding to a chemically reinforced/serum-reduced (Ch-R) medium, to have another formulation for comparison.

In an effort to move toward the direction of generating a clinical-grade product based on IFP-MSCs, we have also reported that compared with FBS-containing media, IFP-MSCs processed in either hPL or Ch-R formulations show enhanced proliferation and multi-differentiation potential [43]. Furthermore, they induce and maintain an intrinsic CD10-rich cellular phenotype, similar to the effect generated with *ex vivo* pro-inflammatory and pro-fibrotic cell priming [18], and are responsible for the efficient Substance P degradation both *in vitro* and *in vivo*. The resulting cell-based product was able to efficiently reverse induced synovitis and IFP fibrosis in a rat model, even at significantly reduced cell numbers [43]. Therefore, manufacturing an IFP-MSC-based cell product with hPL and Ch-R can obviate the use of *ex vivo* cell priming to induce specific phenotypic and functional attributes on the cells.

By contrast, and as mentioned above, we have reported that priming IFP-MSCs with TICs in FBS-containing media significantly enhances their immunomodulatory capacity [18]. Based on this collective information, this study further explored the effects of regulatory-compliant manufacturing conditions (side-by-side comparison with same-donor cells), assessing their phenotypic, molecular and secretory profiles and functionality, with emphasis on the immunomodulatory capacity of IFP-MSCs. We also investigated the response of IFP-MSCs to inflammatory and fibrotic environments when manufactured in different conditions and whether hPL and Ch-R formulations could induce immunomodulatory effects that obviate *ex vivo* cell priming. We found that IFP-MSC expansion in either hPL or Ch-R media results in a significantly increased IFP-MSC immunomodulatory profile compared with FBS-cultured cohorts. These features are indeed further enhanced in all three conditions with concomitant inflammatory and fibrotic priming.

The current comprehensive *in vitro* interrogation improves our understanding of IFP-MSC responses to inflammatory/fibrotic cell priming and whether these intrinsic responses can be induced and/or enhanced by following regulatory-compliant cell-based product manufacturing protocols. The resulting evidence could be harnessed to serve as a foundation for the design of novel and/or to modify existing clinical protocols with IFP-MSC for joint disease including OA based on cell therapy, with potentially more reproducible clinical outcomes.

## Methods

### *Isolation, culture and expansion of IFP-MSCs and bone marrow-derived MSCs*

Human IFP-MSCs were isolated from IFP tissue acquired from de-identified, non-arthritic, age- and sex-matched patients (n = 5, two males and three females, 38.2 ± 12 years old) undergoing elective knee arthroscopy at the Lennar Foundation Medical Center at the University of Miami after obtaining written informed consent. All procedures were carried out in accordance with relevant guidelines and regulations following "not as human research" approval (based on the nature of the samples as discarded tissue) by the University of Miami Institutional Review Board. IFP tissue (5–10 mL) was mechanically dissected and washed repeatedly with Dulbecco's Phosphate-Buffered Saline (DPBS; Sigma Aldrich, St Louis, MO, USA), followed by enzymatic digestion with agitation using 235-U/mL collagenase I (Worthington Industries, Columbus, OH, USA) diluted in DPBS and 1% bovine serum albumin (Sigma Aldrich) for 2 hours at 37°C. Enzymatic digestion was inactivated using complete media with Dulbecco's Modified Eagle's Medium (DMEM) low-glucose GlutaMAX (ThermoFisher Scientific, Waltham, MA, USA) containing 10% FBS (VWR, Radnor, PA, USA), washed and seeded at a density of $1 \times 10^6$ cells/175 $cm^2$ flask in three different complete media: (i) DMEM + 10% FBS, (ii) pooled hPL and (iii) Ch-R. Complete hPL medium was prepared by supplementing DMEM low-glucose GlutaMAX with hPL solution and 0.024 mg/mL xeno-free heparin (PL Bioscience, Aachen, Germany) to obtain a 10% hPL final concentration. Complete Ch-R medium was prepared by mixing low-serum (2% FBS) mesenchymal stem cell growth medium 2 with the provided SupplementMix of defined compounds according to the manufacturer's instructions (PromoCell, Heidelberg, Germany). Forty-eight hours post-seeding, non-adherent cells were removed by gently rinsing with DPBS, and media were replenished accordingly.

All MSCs were cultured at 37°C 5% (v/v) $CO_2$ until 80% confluent as passage 0 (P0), then passaged at a 1:5 ratio until P3, detaching them with TrypLE select enzyme 1X (Gibco, ThermoFisher Scientific) and assessing cell viability with 0.4% (w/v) Trypan Blue (Invitrogen, ThermoFisher Scientific). All experiments were performed using cells obtained from three independent donors (n = 3) unless otherwise specified.

### *TIC priming*

P3 IFP-MSCs expanded in all three culturing conditions were subsequently primed with a TIC inflammatory/fibrotic cocktail (15 ng/mL TNF$\alpha$, 10 ng/mL IFN$\gamma$, 10 ng/mL connective tissue growth factor) for 72 h. Naive and TIC-induced cohorts were evaluated for telomeric, phenotypic, secretory, transcriptional and functional profiles.

### *Telomere length measurement*

A QIAamp DNA mini kit (Qiagen) was used for gDNA extraction from P3 IFP-MSCs expanded in all three culturing conditions. Samples were run in triplicate using 50 ng gDNA for expanded cells. Telomere length measurement by SYBR Green quantitative polymerase chain reaction (qPCR) (#4309155, Invitrogen) involved determining the relative ratio of telomere repeat copy number (T) to a single copy gene (36B4) copy number (S) (T/S ratio) as previously described [44–46].

### *Immunophenotype*

Flow cytometric analysis was performed on P3 non-induced and TIC-primed (n = 3) IFP-MSCs expanded in all three culturing conditions. Briefly, $2.0 \times 10^5$ cells were stained with monoclonal antibodies specific for CD146 (Miltenyi Biotec, Auburn, CA, USA), CD10 (Biolegend, San Diego, CA, USA), human leukocyte antigen (HLA)-DR (BD Biosciences, San Jose, CA), CD283 (TLR3), CD284 (TLR4), CXCR4 (Invitrogen) and the corresponding isotype controls. These markers confirm and complement a previous full panel of surface markers reported in the study by Kouroupis *et al.*[43]. All samples included a Ghost Red 780 Viability Dye (Tonbo Biosciences, San Diego, CA, USA). Data (20 000 events collected) were acquired using a Cytoflex S (Beckman Coulter, Brea, CA, USA) and analyzed using Kaluza analysis software (Beckman Coulter).

### *Real-time qPCR*

RNA extraction was performed using the RNeasy mini kit (Qiagen, Frederick, MD, USA) according to the manufacturer's instructions. Total RNA (1 $\mu$g) was used for reverse transcription using the SuperScript VILO cDNA synthesis kit (Invitrogen).

A qPCR was then performed using a QuantiFast SYBR Green qPCR kit (Qiagen) and a StepOne real-time thermocycler (Applied Biosystems, ThermoFisher Scientific). For each target, human transcript primers were selected using PrimerQuest (Integrated DNA Technologies, San Jose, CA, USA) (see supplementary Table 1). All samples (n = 3) were analyzed in triplicate. Gene expression levels were calculated using the $\Delta\Delta$Ct method and represented as the relative fold change of the primed cohort to the non-induced ( = 1).

A pre-designed 28-gene TaqMan low-density cytokine array (Applied Biosystems) (see supplementary Table 2) was performed (n = 3) using 1000 ng cDNA per IFP-MSC sample and processed using a StepOne real-time thermocycler (Applied Biosystems). Data analysis was performed using DataAssist software v2.0 (Applied Biosystems). Expression levels were calculated using the $\Delta\Delta$Ct method, and values were represented in a heat map of transcript expression levels (with a 34-cycle cutoff point) using the Pearson correlation distance method and complete linkage clustering method between the different samples. Values were also represented in a separate fold change heat map and table as the fold change of the hPL and Ch-R media (sample), both relative to the FBS medium (reference), following $2^{-\Delta Ct}$ = X sample/X reference.

### *Secretome analysis*

Protein arrays of 20 cytokines and 20 angiogenesis-related molecules (RayBio C-series, RayBiotech, Peachtree Corners, GA, USA) were used to determine secreted levels obtained from IFP-MSCs expanded in all three culturing conditions with and without priming. Media alone were also tested in parallel to assess baseline presence of factors to avoid over-quantification. For each population, 1 mL of conditioned media obtained from two donors ($10^5$ IFP-MSCs/well, 12 wells, n = 2 per culturing condition) was prepared and used for each assay following the manufacturer's instructions. Data shown represent 40-second exposure in the FluorChem E chemiluminescence imaging system (ProteinSimple, San Jose, CA, USA). Results were generated by quantifying the mean spot pixel density of each array using a protein array analyzer plugin and ImageJ software (https://imagej.net/Citing). The signal intensities from the average of two spots per protein were normalized with the background signal (including media alone) and quantified by densitometry analysis.

### *Pathway analysis*

Putative interactomes were generated using the Search Tool for the Retrieval of Interacting Genes/Proteins 11.0 (available from: http://string-db.org) [47] database using interaction data from experiments, databases, genome neighborhood, gene fusions, co-occurrence across genomes, co-expression and text-mining. An interaction confidence score of 0.4 was imposed to ensure high interaction probability. The K-means clustering algorithm was used to organize proteins into three separate clusters per condition tested,

discriminated by colors. Venn diagrams were used to demonstrate all possible relations between non-induced and TIC-primed IFP-MSCs cultured in all three conditions for the significantly ($P < 0.05$) altered proteins. Functional enrichments related to biological process, Kyoto Encyclopedia of Genes and Genomes pathways and reactome pathways were presented in radar graphs for all conditions tested.

*Indoleamine-2,3-dioxygenase metabolic activity* in vitro

Indoleamine-2,3-dioxygenase (IDO) activity immunoassay (Abcam, MA, USA) was used to quantify the secreted levels (pg/mL) in expanded IFP-MSCs under all three culture conditions with and without priming ($10^5$ IFP-MSCs/well, 12 wells) following the manufacturer's instructions. The IDO activity kit provides a fluorogenic developer that selectively reacts with N-formylkynurenine to produce a highly fluorescent product. IDO activity was quantified in centrifuged (1500 rpm, 5 minutes) conditioned media (run in duplicates within the membrane) obtained from IFP-MSC cultures in all conditions. Levels were determined by measuring the fluorescence (Ex/Em = 402/488 nm) of individual wells in endpoint mode (SpectraMax M5 spectrophotometer; Molecular Devices, San Jose, CA, USA). IDO metabolic activity (in pmole/min/mg) was obtained by applying the fluorescent values from individual wells to the N-formylkynurenine standard curve run with the assay to obtain the pmole of L-tryptophan metabolized by IDO.

*Prostaglandin E2* in vitro *assay*

The Parameter prostaglandin E2 (PGE2) competitive immunoassay (R&D Systems, MN, USA) was used to quantify the secreted levels (pg/mL) in expanded IFP-MSCs under all three culture conditions with and without priming ($10^5$ IFP-MSCs/well, 12 wells) following the manufacturer's instructions. PGE2 was quantified in conditioned media (run in duplicates within the membrane) obtained from IFP-MSC cultures in all conditions. Levels were determined by subtracting measured optical densities of individual wells at 450 nm and 540 nm in endpoint mode (SpectraMax M5 spectrophotometer; Molecular Devices) and converting into concentrations using the reference standard curve run with the assay.

*Immunopotency assay*

Culture-expanded IFP-MSCs were designated as non-induced or TIC-primed cohorts. After 72 h in complete culture (non-induced) or TIC priming (primed) media, IFP-MSC cultures were washed once with DPBS, and media were changed to an immunopotency assay medium containing RPMI (Gibco) with 15% human AB serum (Corning, Corning, NY, USA), 1% L-glutamine (Gibco), 1% non-essential amino acids (Gibco), 1% sodium pyruvate, 1% N-2-hydroxyethylpiperazine-N-2-ethane sulfonic acid (Gibco) and 1% 100X vitamins (Gibco). Human pan T cells (STEMCELL Technologies, Vancouver, Canada) were stained using the CellTrace carboxyfluorescein succinimidyl ester (CFSE) cell proliferation kit (Invitrogen) according to the manufacturer's instructions and resuspended in immunopotency assay media. Next, CFSE-stained T cells were added to non-induced or TIC-primed IFP-MSCs at a 2:1 ratio. Cell stimulation cocktail 500x (Invitrogen) containing phorbol 12-myristate 13-acetate and ionomycin was then added to the wells designated for T-cell stimulation. After 72 hours, CFSE-stained cells were collected, stained with Ghost Red 780 Viability Dye (Tonbo Biosciences), and acquisition of 10,000 events was performed using a CytoFLEX S cytometer with CytExpert software (Beckman Coulter). T cells were gated by scatter, viability and CFSE positivity, and T-cell proliferation was represented as $CFSE^{dim}$/total CFSE × 100.

*Statistical analysis*

Normal distribution of values was assessed by the Kolmogorov-Smirnov normality test. Statistical analysis was performed using paired and unpaired Student's *t*-test for normally distributed data and Wilcoxon (for paired data) or Mann-Whitney (for unpaired data) test in the presence of a non-normal distribution; one-way ANOVA was used for multiple comparisons. All tests were performed with GraphPad Prism 7.03 (GraphPad Software, San Diego, CA, USA). Statistical significance was set at $P < 0.05$. Data used for the statistical analyses are indicated in the figure legends, corresponding overall to three independent experiments from IFP-MSC donors (n = 3) unless otherwise specified.

## Results

*Cell characterization of IFP-MSCs expanded in all three formulations*

Morphologic differences of IFP-MSCs were observed when cultured in the three culture conditions. IFP-MSCs expanded in either FBS or Ch-R showed a fibroblast-like morphology, while in hPL they exhibited more elongated, spindle-shaped morphology. Consistent with our previous study [43], despite the addition of heparin to the hPL formulation, a thin, fibrin-rich layer formed underneath the cells, potentially affecting their initial adhesive capacity *in vitro*. Nevertheless, they all exhibited comparable sizes and no changes before or after TIC priming (Figure 1A). Full growth kinetics, stemness and differentiation potential of the cells were assessed and reported in the study by Kouroupis *et al.* [43]. Telomere length capacity, as measured by qPCR, showed almost identical T/S ratio for all non-induced and TIC-primed cohorts. The average T/S ratio in non-induced cultures was 1.91, while the average was 1.93 in primed conditions (Figure 1B).

A complete immunophenotypification of IFP-MSCs expanded with the three formulations was recently reported in the study by Kouroupis *et al.* [43]. Here we confirm key markers under priming conditions and further expand the panel with additional ones, including the immune response markers TLR3 and TLR4 (Figure 1C). We confirmed the higher expression of CD146 and CD10 in non-induced IFP-MSCs expanded in either hPL or Ch-R media compared with FBS and their further increase with priming (especially with Ch-R). Of note, CD146 increase with hPL expansion has been previously reported for bone marrow-derived MSCs [48]. Similarly, we confirmed both the absence and significant presence of HLA-DR in non-induced and primed cells, respectively. CXCR4 experienced a similar trend, though this was less pronounced than that seen with HLA-DR, with minimal expression in non-induced IFP-MSCs and an increase after priming. TLR3 was significantly enriched in all non-induced cultures, especially in the hPL and FBS groups (91.2% ± 2.2% and 82.6% ± 28.0%, respectively), whereas TLR4 demonstrated low levels of expression in all non-induced cultures. Interestingly, upon priming, both TLR3 and TLR4 were reduced, though this was more dramatic in TLR3.

*IFP-MSCs expanded in either hPL or Ch-R have a distinguishable transcriptional profile compared with FBS*

A basic transcriptional profile of non-induced IFP-MSCs expanded in either hPL or Ch-R relative to FBS cultures showed similar expression trends for all transcripts tested (Figure 1D). For non-induced IFP-MSCs expanded in hPL, IL-8, CD10 and granulocyte colony-stimulating factor (G-CSF) gene expression was 4.5-, 4.2- and 14.5-fold higher ($P < 0.05$), respectively, than that seen with FBS cultures. For non-induced IFP-MSCs expanded in Ch-R, the same genes were expressed 5.2-, 4.3- and 134.3-fold higher ($P < 0.05$), respectively, than that seen with FBS cultures. All the other transcripts, including IL-6, had lower gene expression in non-induced IFP-MSCs expanded in either hPL or Ch-R compared with FBS cultures, which, when combined with high IL-8 expression, is associated with a significantly low IL-6/IL-8 ratio, suggesting a less pro-inflammatory effect [18,43,49]. Upon priming, all transcripts showed similar overall trends in IFP-MSCs expanded in either hPL or Ch-R relative to FBS cultures (Figure 1D).

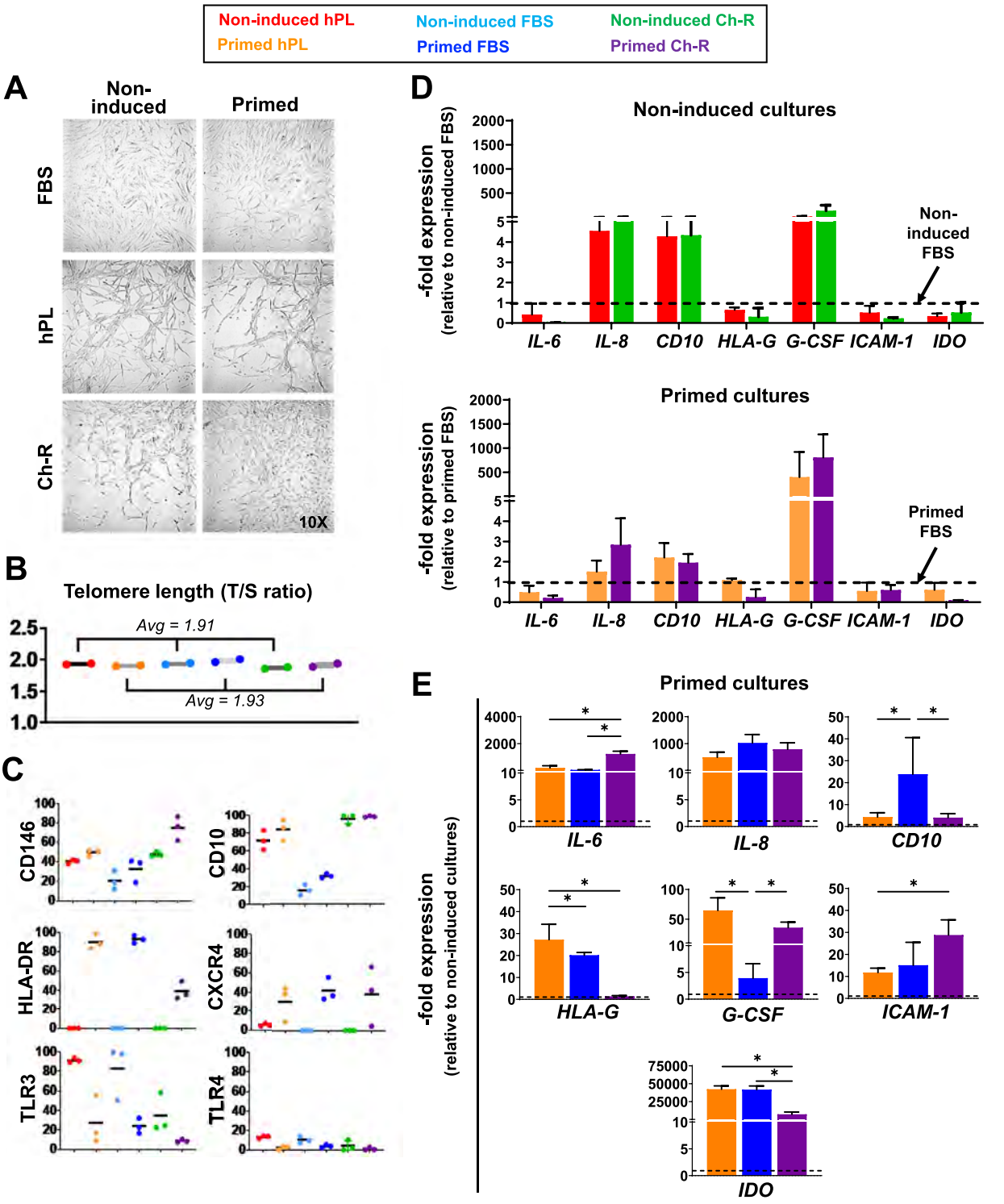


**Fig. 1.** IFP-MSC characterization. (A) IFP-MSCs showed different morphology when expanded in the three different media. Cells expanded in FBS and Ch-R had the characteristic fibroblast-like morphology (the latter smaller in size), while cells expanded in hPL were more spindle-shaped. Of note, despite the addition of heparin to the hPL formulation, a thin fibrin-rich layer formed underneath the expanding IFP-MSC cultures. Magnification 10X. (B) Telomere length, calculated using the ratio of telomere repeats (T) to a single-copy gene 36B4 (S), was similar in the three cultures before and after TIC priming. The average T/S ratio was 1.91 in non-induced cultures and 1.93 in primed cultures. (C) Immunophenotypification showed non-induced IFP-MSCs expanded in either hPL or Ch-R enhanced CD146, CD10 and TLR3 expression. TIC priming further increased CD146 and CD10 and resulted in a sharp increase in HLA-DR in all cultures, while it reduced TLR3 and TLR4 in all cultures. (D) IFP-MSCs expanded in either hPL or Ch-R showed enhanced transcriptional profile with enriched expression of *IL-8*, *CD10* and *G-CSF* genes compared with cohorts expanded in FBS. (E) All immunomodulation-related genes tested showed higher expression levels in the three cultures upon TIC priming compared with non-induced cultures. Of note, HLA-G, G-CSF and IDO showed stronger upregulation in TIC-primed, hPL-expanded IFP-MSCs. All experiments were performed independently (n = 3). Data are presented as scatter plots with mean values and bar plots for transcripts with mean ± SD values. Significant gene expression ($P < 0.05$) differences are marked with an asterisk. Avg, average; SD, standard deviation.

IL-8 and CD10 gene expression was reduced in primed cells compared with non-induced counterparts but remained significantly higher compared with primed IFP-MSCs expanded in FBS. By contrast, G-CSF gene expression was significantly upregulated after priming ($P < 0.05$). For primed IFP-MSCs expanded in hPL, IL-8, CD10 and G-CSF gene expression was 1.5-, 2.2- and 399.6-fold higher ($P < 0.05$), respectively, than that seen with IFP-MSCs expanded in FBS. For primed IFP-MSCs expanded in Ch-R, IL-8, CD10 and G-CSF gene expression was 2.8-, 1.9- and 808-fold higher ($P < 0.05$), respectively, than that seen with IFP-MSCs expanded in FBS. IL-6/IL-8 ratio remained low in primed IFP-MSCs expanded in either hPL or Ch-R compared with FBS.

Upon TIC priming, all transcripts showed similar overall trends in IFP-MSCs expanded in either hPL or Ch-R or FBS relative to their non-induced cultures (Figure 1E). Importantly, HLA-G and IDO gene expression showed stronger upregulation in hPL or FBS compared with Ch-R TIC-primed IFP-MSC cultures. Also, G-CSF gene expression was upregulated more significantly ($P < 0.05$) in TIC-primed hPL or Ch-R, whereas CD10 was increased more significantly ($P < 0.05$) in TIC-primed, FBS-expanded IFP-MSCs.

To complement the above profile, a pre-designed cytokine multiplex array was used to investigate the overall inflammation-related molecular signature of IFP-MSCs processed in all three conditions and subjected to TIC priming. Overall, TaqMan low-density cytokine array analysis results showed that TIC-primed IFP-MSCs expanded in either hPL and Ch-R have low to negative expression levels (marked blue or white on the heat map) for most inflammation-related cytokines tested (Figure 2A). Only four molecules showed significantly ($\geq$ 2-fold, $P < 0.05$) higher expression levels in hPL-expanded IFP-MSCs—IFN-$\alpha$-1, IFN-$\alpha$-8, IL-1-$\alpha$ and IL-1-$\beta$—compared with the FBS reference sample, with 2.4-fold, 2.1-fold, 4.8-fold and 2.2-fold expression levels, respectively. Ch-R-expanded IFP-MSCs had significantly ($\geq$ 2-fold, $P < 0.05$) higher expression of six transcripts—IFN-$\alpha$-1, IFN-$\alpha$-8, IL-1-$\alpha$, IL-1-$\beta$, IL-8 and TNF$\alpha$—compared with the FBS reference sample, with 7.7-fold, 4.7-fold, 30.4-fold, 351.8-fold, 9.0-fold and 10.3-fold expression levels, respectively. Importantly, two genes (IL-12A coding for IL-12-$\alpha$ and IL-18) showed commonly reduced expression levels in IFP-MSCs expanded in either hPL or Ch-R compared with cohorts expanded in FBS (Figure 2B).

### *IFP-MSCs expanded in either hPL or Ch-R exhibit a robust secretion of cytokines and angiogenesis-related factors with and without priming*

Non-induced IFP-MSCs expanded in either hPL or Ch-R showed overall higher secretion of cytokines and angiogenesis-related factors compared with cohorts expanded in FBS (Figure 3A). Among 40 secreted proteins tested, 21 were secreted in significantly ($P < 0.05$) higher amounts in hPL-expanded IFP-MSCs. Among the highly secreted proteins in primed IFP-MSCs expanded in hPL are eotaxin-1, eotaxin-2, G-CSF, IL-6, IL-7, IL-8, IL-10, angiogenin, EGF, CXCL5, bFGF, GRO, IFN-$\gamma$, leptin, MCP-1, PDGF-BB, PLGF, CCL5, TGF-$\beta$1, THPO and vascular endothelial growth factor (VEGF)-A. Non-induced IFP-MSCs expanded in Ch-R had significantly ($P< 0.05$) higher secretion of 14 proteins, with only three molecules (insulinlike growth factor 1, IL-6, VEGF-D) showing lower secretion levels compared with FBS-expanded IFP-MSCs (Figure 3A).

TIC priming resulted in increased secretion of various proteins for IFP-MSCs expanded in either hPL or Ch-R (Figure 3B). In IFP-MSCs expanded in hPL, 15 proteins had higher secretion levels compared with cohorts expanded in FBS. Among the highly secreted proteins in primed IFP-MSCs expanded in hPL are IL-2, IL-7, IL-8, IL-10, IL-11, I-309, EGF, CXCL5, GRO, IFN-$\gamma$, MCP-1, PDGF-BB, PLGF, TIMP-1 and VEGF-A. In IFP-MSCs expanded in Ch-R, 19 proteins had higher and three (IFN-$\gamma$, PLGF, TGF-$\beta$1) had lower secretion levels compared with cohorts expanded in FBS (Figure 3B).

### *Highly secreted cytokines and angiogenesis-related factors in IFP-MSCs expanded in either hPL or Ch-R show strong protein-protein interaction enrichment*

To assess the relationship among proteins for statistically significant differences ($P < 0.05$) between all three conditions in non-induced and TIC-primed cells, protein association network analysis was performed using the Search Tool for the Retrieval of Interacting Genes/Proteins 11.0 software. In general, all secreted proteins appeared interconnected, at least through one association, and according to the K-means clustering algorithm could be clustered into three groups, each one representing highly interactive proteins (Figure 3B). All K-means clustering networks demonstrated elevated protein-protein interaction enrichment ($P < 1.0e-16$) and an average local clustering coefficient $> 0.7$, indicating that the proteins used were at least partially biologically connected. Venn diagram analysis was used to compare the secretion profiles between non-induced and TIC-primed IFP-MSCs expanded in either hPL or Ch-R (Figure 3C). In non-induced IFP-MSCs, out of 21 proteins for hPL- and 14 for Ch-R-expanded cells that were significantly ($P< 0.05$) different from the FBS cohorts, the majority (13 proteins, 62%) were common. Those shared proteins were eotaxin-2, G-CSF, angiogenin, CCL5, IFN-$\gamma$, IL-8, IL-10, CXCL1, CXCL5, MCP-1, bFGF, leptin and THPO. This difference in secretory profile of IFP-MSCs expanded in either hPL or Ch-R indicates that hPL medium significantly enhances the secretion behavior of non-induced IFP-MSCs. TIC priming resulted in an increase in the shared proteins (12 proteins, approximately 63–80%) between TIC-primed IFP-MSCs expanded in either hPL or Ch-R. Those shared proteins were IL-2, IL-7, IL-8, IL-10, IL-11, EGF, PDGF-BB, VEGF-A, CXCL1, CXCL5, MCP-1 and TIMP-1. Additionally, TIC priming increased the secreted quantity of proteins present only in moderate levels in non-induced IFP-MSCs expanded in either FBS or Ch-R (Figure 3C,D).

Simultaneous Venn diagram representation of all four different secretory profiles—namely, non-induced/TIC-primed hPL and non-induced/TIC-primed Ch-R media—revealed a “core” of five proteins (IL-8, IL-10, CXCL1, CXCL5, MCP-1) common between them (Figure 3C). Six biological processes were evaluated; namely, regulation of cell proliferation (GO:0042127), positive regulation of response to stimulus (GO:0048584), positive regulation of cell migration (GO:0030335), positive regulation of protein phosphorylation (GO:0001934), positive regulation of vasculature development (GO:1904018) and regulation of signaling receptor activity (GO:0010469) (Figure 3E, upper radar graph). In non-induced IFP-MSCs, expansion in either hPL or Ch-R media revealed similar biological processes, except for positive regulation of cell migration and vasculature development processes, which showed significantly lower involvement or outright absence in IFP-MSCs expanded in Ch-R. Interestingly, TIC priming significantly increased (from 0% to 31.5%) positive regulation of the vasculature development process in IFP-MSCs expanded in Ch-R, whereas in IFP-MSCs expanded in hPL, reduced positive regulation of cell migration, protein phosphorylation and vasculature development were noted. Additionally, eight Kyoto Encyclopedia of Genes and Genomes and reactome pathways were evaluated: cytokine-cytokine receptor interaction (hsa:04060), MAPK signaling (hsa:04010), PI3K-Akt signaling (hsa:04151), Ras signaling (hsa:04014), Jak-STAT signaling (has:04630), Rap1 signaling (has:04015), signaling by interleukins (HSA: 449147) and interleukin-10 signaling (HSA: 6783783) (Figure 3E, bottom radar graph). Overall, in the non-induced state, IFP-MSCs expanded in hPL showed protein involvement in all of the above-mentioned pathways, whereas in Ch-R protein involvement in four out of eight pathways was totally absent. Interestingly, TIC priming resulted in a similar number of proteins involved in the eight pathways tested for IFP-MSCs expanded in either hPL or Ch-R (Figure 3E, bottom radar graph).

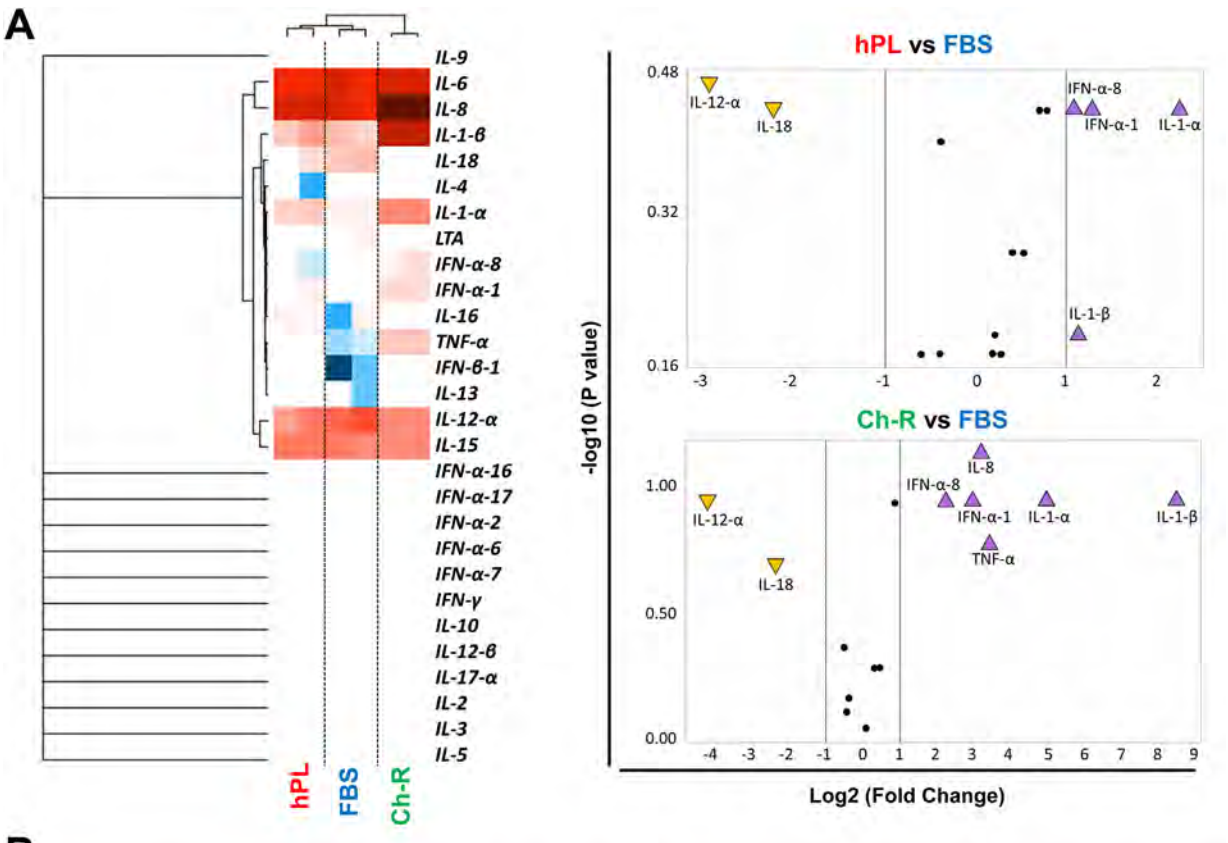


B

| Gene name | FBS | hPL / FBS (fold change) | Ch-D / FBS (fold change) |
|---|---|---|---|
| IFN-α-1 | 1 | 2.4 | 7.7 |
| IFN-α-16 | 1 | 1.6 | 1.8 |
| IFN-α-17 | 1 | 1.6 | 1.8 |
| IFN-α-2 | 1 | 1.6 | 1.8 |
| IFN-α-6 | 1 | 1.6 | 1.8 |
| IFN-α-7 | 1 | 1.6 | 1.8 |
| IFN-α-8 | 1 | 2.1 | 4.7 |
| IFN-β-1 | 1 | 1.2 | 1.3 |
| IFN-γ | 1 | 1.6 | 1.8 |
| IL-10 | 1 | 1.6 | 1.8 |
| IL-12-α | 1 | 0.2 | 0.2 |
| IL-12-β | 1 | 1.6 | 1.8 |
| IL-13 | 1 | 1.2 | 1.3 |
| IL-15 | 1 | 1.2 | 0.7 |

| Gene name | FBS | hPL / FBS (fold change) | Ch-D / FBS (fold change) |
|---|---|---|---|
| IL-16 | 1 | 1.4 | 0.8 |
| IL-17-α | 1 | 1.6 | 1.8 |
| IL-18 | 1 | 0.1 | 0.1 |
| IL-1-α | 1 | 4.8 | 30.4 |
| IL-1-β | 1 | 2.2 | 351.8 |
| IL-2 | 1 | 1.6 | 1.8 |
| IL-3 | 1 | 1.6 | 1.8 |
| IL-4 | 1 | 1.7 | 1.8 |
| IL-5 | 1 | 1.6 | 1.8 |
| IL-6 | 1 | 0.8 | 1.1 |
| IL-8 | 1 | 1.3 | 9.0 |
| IL-9 | 1 | 1.6 | 1.8 |
| LTA | 1 | 0.7 | 0.7 |
| TNF-α | 1 | 0.8 | 10.3 |

**Fig. 2.** Effect of TIC priming on IFP-MSC inflammation-related transcriptome. (A) Pre-designed cytokine multiplex array showing that IFP-MSCs expanded in either hPL or Ch-R had a comparable transcriptional profile upon TIC priming. TIC-primed hPL- and Ch-R-expanded IFP-MSCs had low to negative expression levels (marked blue or white on the heat map) for most inflammation-related cytokines tested. Only four molecules for hPL- and six for Ch-R-expanded IFP-MSCs showed significantly (≥ 2-fold, $P < 0.05$) higher expression levels compared with the FBS reference sample. Two molecules (IL-12-α and IL-18) showed commonly reduced expression levels in hPL- and Ch-R-expanded IFP-MSCs compared with FBS. (B) Table shows the fold change difference in transcript expression between hPL or Ch-R and the FBS reference sample. All experiments were performed independently (n = 2). Data are presented as volcano plots and scatter plots with mean values.

*IFP-MSCs expanded in either hPL or Ch-R show increased immunomodulatory function* in vitro

Non-induced IFP-MSCs expanded in either hPL or Ch-R showed significantly ($P < 0.05$) higher IDO activity compared with FBS cultures (1.5-fold and 1.6-fold, respectively) (Figure 4A). As expected, upon TIC priming, IDO activity was similarly increased in all three cultures, resulting in comparable high levels (average 1000 $\mu$U/mg). Interestingly, PGE2 showed significantly higher secreted levels in non-induced IFP-MSCs expanded in hPL (318.4 ± 95 pg/mL, $P < 0.05$) compared with IFP-MSCs expanded in either Ch-R FBS or Ch-R (6-fold and 14-fold, respectively). Similarly, TIC priming resulted in higher secreted levels of PGE2 for all three cultures (Figure 4B).

IFP-MSCs expanded in either hPL or Ch-R showed increased immunomodulatory capacity in IFP-MSC/T-cell immunopotency co-cultures. Exposure of non-induced IFP-MSCs to activated T cells resulted in an increased spindle-shaped morphology for all three cultures, which was more pronounced when cultures were TIC-primed and co-cultured with non-induced or activated T cells (Figure 5A). Importantly, only non-induced IFP-MSCs expanded in either hPL or Ch-R attenuated activated T-cell proliferation (5% and 24%, respectively, $P < 0.05$) when compared with IFP-MSCs expanded in FBS. TIC priming resulted in increased reduction of activated T-cell

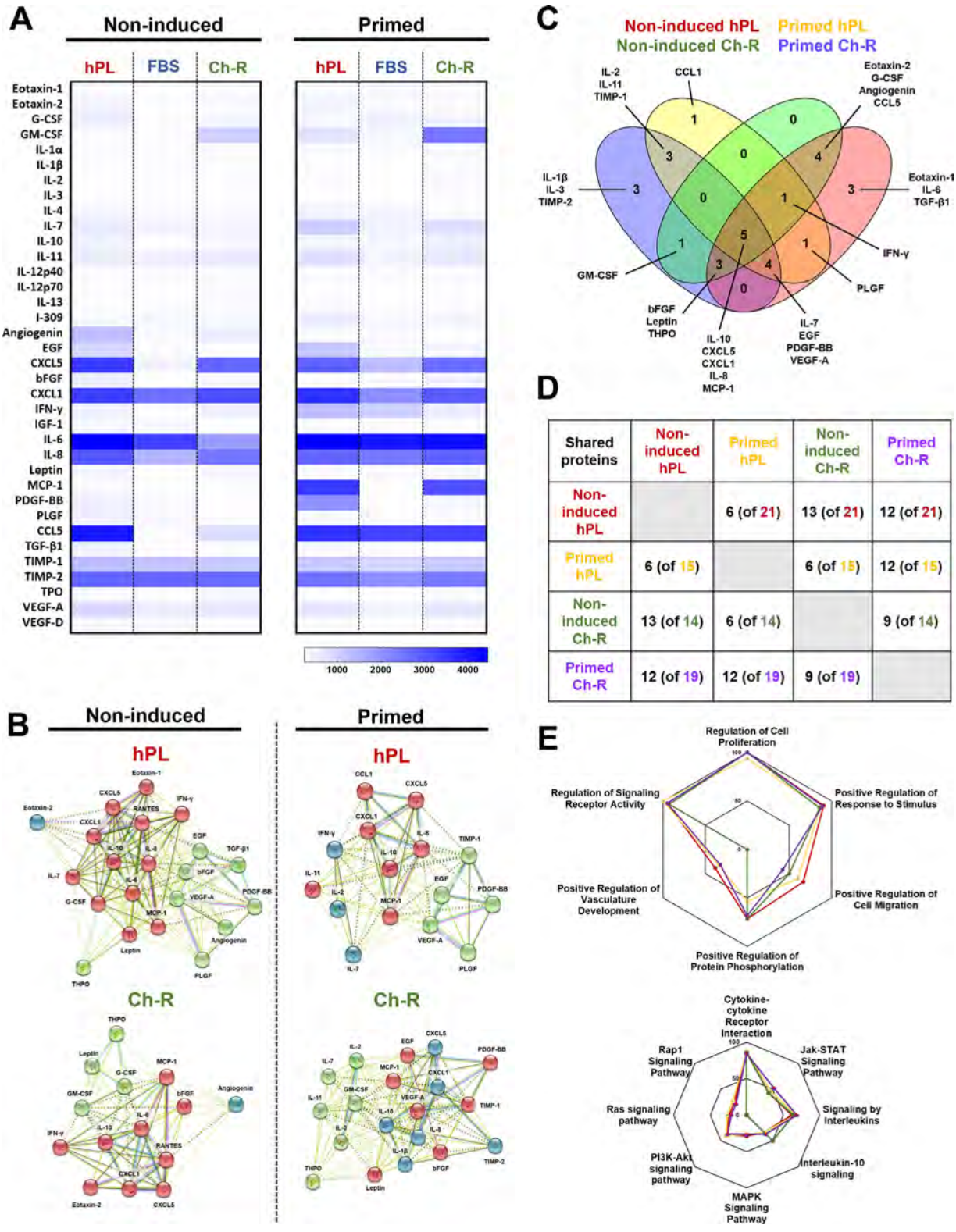


**Fig. 3.** Secretory profiling of non-induced and TIC-primed IFP-MSC cultures. (A) Secretory profile heat maps of non-induced and TIC-primed IFP-MSCs and indicated immunomodulatory/pro-angiogenic factor secretion for IFP-MSCs expanded in either hPL or Ch-R. Heat map colors are assigned according to a molecule concentration relative scale, from 0 to 10 000. (B) STRING analysis of the proteins with statistical differences between either hPL or Ch-R groups and FBS for both non-induced and TIC priming conditions (total of 40) was performed using all available interaction sources and 0.4 as a confidence interaction score. K-means algorithm revealed high PPI enrichment ($P < 1.0e-16$), with all proteins clustered into three groups, indicated by different colors. (C) Venn diagram showing shared proteins among all groups (statistically significant difference from FBS/non-induced or FBS/priming). Except the "core" of the immunomodulatory/angiogenic proteins present in non-induced cultures (IL-8, IL-10, CXCL1, CXCL5, MCP-1), TIC-primed IFP-MSCs expanded in either hPL or Ch-R additionally showed common secretion of seven other proteins (IL-2, IL-7, IL-11, TIMP-1, EGF, PDGF-BB, VEGF-A). (D) Table shows the number of proteins shared by different groups and conditions. (E) Six biological processes and eight KEGG/reactome pathways were evaluated. In non-induced IFP-MSCs, hPL and Ch-R media showed similar biological processes, except positive regulation of cell migration and vasculature development processes, which were significantly less involved or absent in IFP-MSCs expanded in Ch-R. Non-induced IFP-MSCs expanded in hPL showed protein involvement in all KEGG/reactome pathways, whereas non-induced IFP-MSCs expanded in Ch-R showed totally absent protein involvement in four out of eight pathways. All experiments were performed independently (n = 2). KEGG, Kyoto Encyclopedia of Genes and Genomes; PPI, protein-protein interaction; STRING, Search Tool for the Retrieval of Interacting Genes/Proteins.

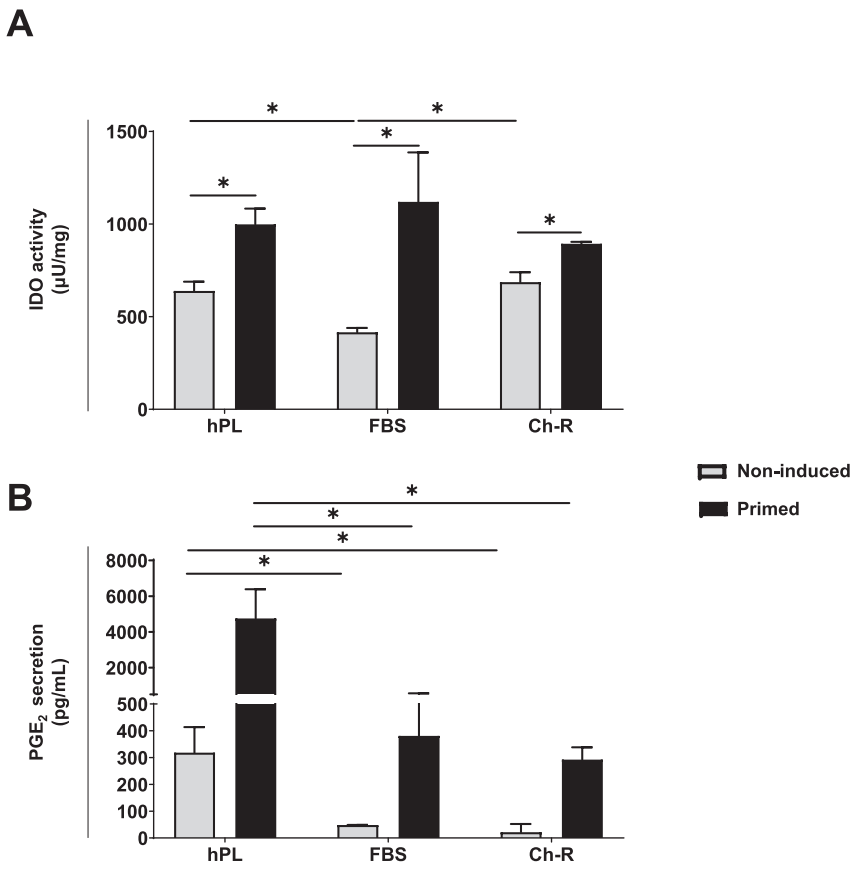


**Fig. 4.** IDO activity and PGE2 secretion levels in non-induced and TIC-primed IFP-MSCs. (A) Non-induced IFP-MSCs expanded in either hPL or Ch-R showed significantly ($P < 0.05$) higher IDO activity compared with cohorts expanded in FBS. (B) PGE2 showed significantly ($P < 0.05$) higher secreted levels in non-induced cells expanded in hPL (318.4 ± 95 pg/mL) compared with both FBS and Ch-R groups. (A and B) Upon TIC priming, IDO activity and PGE2 secretion were increased in all three IFP-MSC cultures, especially hPL for PGE2. All experiments were performed independently (n = 3). Data are presented as bar plots with mean ± SD values. SD, standard deviation.

proliferation for all three cultures (on average, 19% for FBS, 28% for hPL and 37% for Ch-R; $P < 0.05$) (Figure 5B).

## Discussion

In our previous studies, we demonstrated that IFP-MSCs cultured in FBS-containing media are capable of degrading Substance P both *in vitro* and *in vivo* via CD10 enrichment while showing an intrinsic immunomodulatory effect suppressing the proliferation of activated PBMCs, all of whose capacities are particularly enhanced with prior inflammatory/fibrotic (i.e., TIC) cell priming [18]. Moreover, we demonstrated [43] that manufacturing an IFP-MSC cell product incorporating regulatory-compliant practices (i.e., replacing FBS media supplementation with hPL) or reducing FBS and adding recombinant proteins (i.e., Ch-R) obviates the need for cell priming to induce an effective CD10-rich phenotype still capable of efficiently degrading Substance P *in vitro* and *in vivo*. Based on this consistent evidence, we investigated the immunomodulatory profile and functional capacity of IFP-MSCs processed under similar manufacturing conditions. We also tested their response to inflammatory/fibrotic pathological environments, such as the ones present in a diseased joint, helping to anticipate their functional changes after intra-articular administration. Our findings contribute relevant information on the benefits of manufacturing IFP-MSCs with either hPL or Ch-R compared with traditional FBS-supplemented media. The collective findings provide evidence of such manufacturing conditions resulting in phenotypic, transcriptional and secretory profiles that translate into superior immunomodulatory effects. We show an enhanced response in cells processed in all three manufacturing conditions when exposed to inflammatory/fibrotic conditions, though, again, this is more pronounced in cells expanded with either hPL or Ch-R.

IFP-MSCs constitute an interesting cellular alternative for cell-based therapy for joint disease [10–14] given their intrinsic and scalable properties. These include high cell yields per volume of tissue (as with other adipose-derived MSCs), higher proliferative and differentiation potential compared with other MSC types (e.g., bone marrow-derived) [16,17], immunomodulatory capacity and degradative activities over local key molecules in joint disease [18,43]. On the other hand, their intra-articular origin may not only support the view that they are "homologous" from a regulatory perspective (when intended for a similar intra-articular therapy) but may also equip them with innate features and attributes as part of the IFP/synovium complex [3] and thus as active participants in joint homeostasis and the potential establishment and progression of joint disease, including OA [4–8].

Successful and reproducible clinical outcomes in cell-based therapy largely depend on reducing the variability of the manufactured cellular product under regulatory-compliant practices. Based on this, efforts have been centered around the generation of clinically relevant cell numbers under specific conditions that support MSC proliferation without compromising viability while also preserving and/or enhancing their functional attributes. FBS-containing media have been widely used in MSC production for clinical trials, yet research has shown that exposure to FBS significantly increases the risk of viral transmission and immune reaction complications upon transplantation *in vivo*. Specifically, antigens present in animal serum can be internalized by cultured-expanded MSCs in the range of 7–30 mg of protein with a standard preparation of 100 million human MSCs [50]. As a potential solution, serum-reduced and serum-free, chemically reinforced media formulations have been developed and are

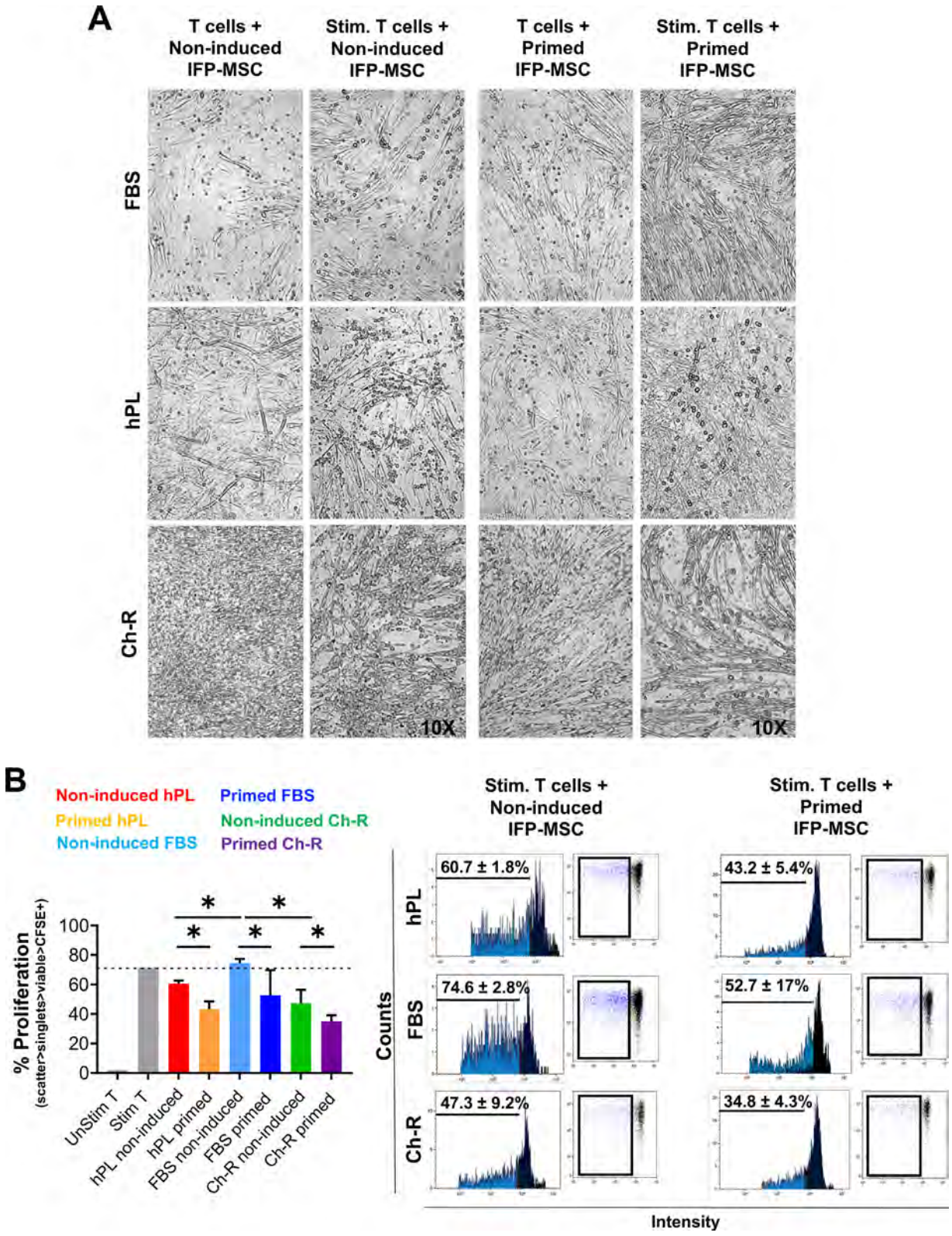


**Fig. 5.** IFP-MSCs expanded in either hPL or Ch-R showed increased immunomodulatory functionality in immunopotency assay. (A) Exposure of non-induced IFP-MSCs to PMA/IO-activated T cells resulted in an increased spindle-shaped morphology for all three cultures that was more pronounced when cultures were TIC-primed and co-cultured with non-induced or PMA/IO-activated T cells. Magnification 10X. Pictures taken at the end of the 72-h co-stimulation. (B) Unlike IFP-MSCs expanded in FBS, non-induced cells expanded in either hPL or Ch-R abrogated PMA/IO-activated T-cell proliferation. This effect was further enhanced with TIC priming in all three cultures. All experiments were performed independently (n = 3). Data are presented as bar plots with mean ± SD values and flow cytometry histograms, with gated (rectangle) T-cell progenies generated in cultures upon PMA/IO activation. Significant T-cell proliferation ($P < 0.05$) differences are marked with an asterisk. IO, ionomycin; PMA, phorbol 12-myristate 13-acetate; SD, standard deviation; Stim, stimulated.

currently commercially available. Despite promising results, their use in MSC culturing still yields variable outcomes in terms of proliferative responses and functionality *in vitro* [51,52], largely dependent on the final composition of the medium, which is often undisclosed by the manufacturer. By contrast, hPL has grown as a viable regulatory-compliant alternative for the supplementation of MSC expansion. Beyond the established effects on cell growth, previous studies have shown that hPL contains a series of bioactive molecules, which include growth factors, chemokines and adhesion molecules (reviewed by Burnouf *et al.* [53]), that can "prime" MSCs to acquire an immunomodulatory phenotype, as we demonstrate here for IFP-MSCs. However, regulatory agencies are becoming more stringent in terms of hPL composition, origin, characteristics and quality controls. Consequently, to ensure the quality and safety of hPL supplements, minimal requirements have been delineated related to the source of platelet concentrates, donor variability, number of donors in pooled preparations, manufacturing processes and pathogen-free safety measures (reviewed by Schallmoser *et al.* [54]).

IFP-MSC cultures showed significant differences in shape and size for all three conditions. However, these morphological differences were not reflected in alterations in telomere dynamics, a reported outcome of "*in vitro* MSC aging" [44–46], as in all non-induced and TIC-primed cells the T/S ratios were comparable. Importantly, short-term exposure to inflammatory/fibrotic (i.e., TIC) conditions had no detrimental effect on telomere lengths in any conditions. Specifically, the average telomere length of IFP-MSCs (passage 3) in both non-induced and TIC-primed cultures was 7.8 kb, which is comparable to previously reported telomere measurements from cultured synovium-derived MSCs (7.08 kb) [55]. This finding is important, as it indicates that MSCs isolated from anatomical neighboring tissues (i.e., IFP and synovium) show comparable telomere dynamics *in vitro* irrespective of the expansion conditions.

Both hPL and Ch-R formulations induced a baseline phenotype in non-induced IFP-MSC and further enriched in primed cohorts, with specific markers (e.g., CD146 and CD10) previously associated with different functionalities in adipose-derived MSC and IFP-MSC including chondrogenic differentiation and immunomodulation [18,56–59]. These findings support previous reports with other types of MSCs (bone marrow-derived), in which CD146 expression increases specifically with hPL expansion [48]. Additionally, TLR3 was significantly enriched, whereas TLR4 showed low levels of expression in all non-induced cultures and priming uniformly reduced their expression across all formulations, suggesting negative feedbacks intended to regulate their "sensitivity" to injury/inflammation-related factors.

Even though MSCs traditionally show high inherent variability upon expansion *in vitro*, the transcriptional profiling of non-induced IFP-MSC cultures revealed at least 4-fold higher IL-8, CD10 and G-CSF expression for both hPL- and Ch-R-expanded IFP-MSCs compared with FBS cultures. Their significantly higher expression levels indicate that both hPL- and Ch-R-expanded IFP-MSCs possess enhanced immunomodulatory capacity. The overall secretory response upon expansion in non-induced hPL and Ch-R cultures when compared with FBS cultures involves an enhanced secretion of a wide spectrum of immunomodulatory and angiogenic proteins, including eotaxin-2, G-CSF, CCL5, IFN-$\gamma$, IL-8, IL-10, CXCL1, CXCL5, MCP-1, angiogenin, bFGF, leptin and THPO. Physiologically, all of these molecules are actively released in the *in vivo* microenvironment upon inflammatory stimulation and orchestrate the tissue regeneration process by inhibiting leukocyte transmigration, enhancing angiogenesis and increasing progenitor cell migration and differentiation [60]. Specifically, CXCL1, CXCL5 and IL-8 chemokines are potent ligands for CXCR1 and/or CXCR2 receptors present within immune cells (including neutrophils and monocytes) and endothelial cells, which, via the CXCLs/CXCR2 axis, induce the migration of immune cells and parallel angiogenesis [61]. Additionally, when highly secreted, IL-10 and G-CSF anti-inflammatory cytokines can induce macrophage polarization toward an M2 anti-inflammatory and immunomodulatory state, which in turn, via elevated secretion of IL-10 and TGF-$\beta$, suppresses inflammation and contributes to tissue repair and remodeling, vasculogenesis and restoration of homeostasis [62–64]. A recent study indicated that IL-8, MCP-1, angiogenin and VEGF are highly secreted MSC pro-angiogenic factors involved in migration and tube formation of endothelial cells both *in vitro* and *in vivo* [65]. Interestingly, in our study, three out of these four factors showed enhanced secretion in non-induced hPL and Ch-R cultures compared with FBS cultures. Elevated THPO and leptin secretion observed in non-induced hPL and Ch-R cultures has also been associated with increased angiogenesis. Specifically, THPO secretion stimulates endothelial cell motility and angiogenesis via a platelet-activating factor-dependent mechanism [66], whereas leptin increases endothelial cell proliferation and matrix metalloproteinase production [67].

IFP-MSC exposure to inflammatory/fibrotic conditions resulted in increased secretion of proteins associated with both the inflammatory controlling cascade and angiogenic response in all three culture conditions. Interestingly, with the exception of the "core" of the immunomodulatory/angiogenic proteins present in non-induced cultures (IL-8, IL-10, CXCL1, CXCL5 and MCP-1), TIC-primed IFP-MSCs expanded in either hPL or Ch-R demonstrated common homogeneous secretion between MSC donors of seven additional proteins (IL-2, IL-7, IL-11, TIMP-1, EGF, PDGF-BB and VEGF-A). These factors play key roles during injury and repair. Interleukins, and especially the highly secreted IL-2 and IL-7, are also involved in immunomodulation, as IL-2 regulates the generation and functionality of both T effectors and T regulators, whereas IL-7 affects the generation of naive T cells and the maintenance of memory cells [68]. Pro-angiogenic factors, including EGF, PDGF-BB and VEGF-A [69,70], were highly secreted in TIC-primed IFP-MSCs expanded in either hPL or Ch-R, which can be putatively counterbalanced by the anti-angiogenic activity of secreted TIMPs [71]. Therefore, TIC priming further increased the immunomodulatory and angiogenic functionality in all IFP-MSC cultures. In terms of resulting affected biological processes, various categories were observed to be affected by IFP-MSCs expanded in either hPL or Ch-R, including cell proliferation, response to stimulus, cell migration, protein phosphorylation, vasculogenesis and signaling receptor activity. Combined, the positive effects show how IFP-MSCs respond to inflammation/injury: by increasing their population, migrating to active sites of damage and altering key cascades known to affect local immune responses and vascular remodeling. Interestingly, hPL formulation had a more pronounced effect on both phenomena (even in a non-induced state), while Ch-R had an effect on only the former, mainly due to the low secretion of EGF, PDGF-BB and VEGF-A pro-angiogenic factors.

Previous studies have shown that upon exposure to inflammatory cues such as IFN$\gamma$, TNF$\alpha$ and IL-1$\beta$, MSCs readily increase their secretion of major immunomodulatory mediators, such as the tryptophan-catabolizing enzyme IDO and the soluble factor PGE2 [72,73]. In our study, non-induced IFP-MSCs expanded in either hPL or Ch-R demonstrated significantly higher intrinsic IDO activity compared with FBS. By contrast, only hPL was associated with high PGE2 secretion in non-induced cells (further significantly amplified with TIC priming), suggesting that PGE2-inducing factors are present exclusively in hPL and absent in FBS. These results underline the innate and efficient "priming" effect exerted by hPL on IFP-MSCs, supporting the avoidance of non-compliant *ex vivo* cell priming in acquiring a strong immunomodulatory phenotype in IFP-MSCs. The significance of enhanced IDO activity and high PGE2 levels to induce an immunomodulatory function is consistent with numerous studies in both innate and adaptive immunity. For instance, it has been shown that MSCs can direct monocyte differentiation toward an alternative activation, resulting in an IL-10-producing M2 macrophage phenotype as well as modulation and activation of lymphocyte subsets through IDO activity and the secretion of PGE2 and IL-6 [74–77]. In

addition, MSCs suppress recruited T cells by IDO release within short distances [78], whereas they inhibit $CD4^+$ T-cell differentiation to effector Th17 subtype via a PGE2-dependent cell-cell contact manner [79]. By contrast, the increased levels of secreted IDO and PGE2 molecules in non-induced hPL- and Ch-R-expanded IFP-MSCs were directly related to their immunomodulatory capacity in IFP-MSC/T-cell immunopotency co-cultures. Moreover, only non-induced hPL- and Ch-R-expanded IFP-MSCs could abrogate activated T-cell proliferation *in vitro*, indicating their strong intrinsic anti-inflammatory phenotype. Exposure of all IFP-MSC cultures to synovitis-mimicking priming resulted, as expected, in enhanced abrogation of T-cell proliferation. However, even though MSC/T-cell immunopotency co-culture assay has been widely used to evaluate MSC immunosuppressive potential *in vitro*, it cannot solely predict *in vivo* MSC immunomodulatory capacity, which has to be further validated in relevant pre-clinical animal models.

Collectively, the data suggest to us that the use of a regulatory-compliant media supplement such as hPL and formulations involving serum reduction and addition of recombinant proteins (i.e., Ch-R) obviates the inflammatory cell priming that was once thought to be required to induce a potent immunomodulatory state in MSCs. Given the untoward effects of such priming protocols in terms of HLA-DR expression, potentially inducing alloreactive responses in allogeneic schemes, these findings help alleviate these concerns while permitting the design of effective clinical protocols for the use of IFP-MSC products for joint disease, including OA. The comparable effects observed with hPL and Ch-R in various (not all) outcomes underscore the role of recombinant proteins in the latter, yet the presence of FBS, even in reduced quantities, remains a challenge for translational purposes.

In summary, IFP-MSCs expanded in either hPL or Ch-R result in a cell-based product that possesses MSC-related immunomodulatory phenotypic and transcriptional profiles, enhanced immunomodulatory/pro-angiogenic factor secretion capacity and an enhanced immunomodulatory functional cell signature. Based on this, the enhancement of IFP-MSC therapeutic properties, when manufactured under regulatory-compliant conditions such as hPL, facilitates the translation of proof-of-concept data into potential clinical protocols.

## Funding

The authors are in gratitude with the Soffer Family Foundation and the DRI Foundation for their generous funding support. These funding sources were not involved in any step of the study design, collection, analysis, or interpretation of the data, or writing of the manuscript.

## Declaration Of Competing Interest

DC is a paid consultant of Lipogems USA, LLC, and Cryovida Banco de Células Madre Adultas.

## Author Contributions

Conception and design of the study: DK, ACB, DNG, CL, TMB, LDK and DC. Acquisition of data: DK, ACB, DNG, CL, TMB, LDK and DC. Analysis and interpretation of data: DK, ACB, DNG, CL, TMB, LDK and DC. Drafting or revising the manuscript: DK, ACB, DNG, CL, TMB, LDK and DC. All authors have approved the final article.

## Acknowledgments

The authors thank Melissa Willman for her help with the immunopotency assay as well as the Soffer Family Foundation (DK, ACB, TMB, LDK and DC), the DRI Foundation (DC) and Cryovida Banco de Células Madre Adultas (CL) for their generous funding support.

## Supplementary materials

Supplementary material associated with this article can be found in the online version at doi:10.1016/j.jcyt.2020.06.007.

## References

[1] Gallagher J, Tierney P, Murray P, O'Brien M. The infrapatellar fat pad: anatomy and clinical correlations. Knee Surg Sports Traumatol Arthrosc 2005;13:268–72.
[2] Bohnsack M, Wilharm A, Hurschler C, Rühmann O, Stukenborg-Colsman C, Wirth CJ. Biomechanical and kinematic influences of a total infrapatellar fat pad resection on the knee. Am J Sports Med 2004;32:1873–80.
[3] Macchi V, Stocco E, Stecco C, Belluzzi E, Favero M, Porzionato A, et al. The infrapatellar fat pad and the synovial membrane: an anatomo-functional unit. J Anat 2018;233:146–54.
[4] Clockaerts S, Bastiaansen-Jenniskens YM, Runhaar J, van Osch GJVM, Van Offel JF, Verhaar JAN, et al. The infrapatellar fat pad should be considered as an active osteoarthritic joint tissue: a narrative review. Osteoarthr Cartil 2010;18:876–82.
[5] Barboza E, Hudson J, Chang WP, Kovats S, Towner RA, Silasi-Mansat R, et al. Profibrotic infrapatellar fat pad remodeling without M1 macrophage polarization precedes knee osteoarthritis in mice with diet-induced obesity. Arthritis Rheumatol 2017;69:1221–32.
[6] Gross J-B, Guillaume C, Gegout-Pottie P, Reboul P, Jouzeau J-Y, Mainard D, et al. The infrapatellar fat pad induces inflammatory and degradative effects in articular cells but not through leptin or adiponectin. Clin Exp Rheumatol 2017;35:53–60.
[7] Ioan-Facsinay A, Kloppenburg M. An emerging player in knee osteoarthritis: the infrapatellar fat pad. Arthritis Res Ther 2013;15:225.
[8] Ioan-Facsinay A, Kloppenburg M. Osteoarthritis: Inflammation and fibrosis in adipose tissue of osteoarthritic joints. Nat Rev Rheumatol 2017;13:325–6.
[9] Caplan AI, Correa D. The MSC: an injury drugstore. 2011;9:11–5.
[10] Tangchitphisut P, Srikaew N, Numhom S, Tangprasittipap A, Woratanarat P, Wongsak S, et al. Infrapatellar fat pad: an alternative source of adipose-derived mesenchymal stem cells. Arthritis 2016;2016. 4019873–10.
[11] Hindle P, Khan N, Biant L, Péault B. The infrapatellar fat pad as a source of perivascular stem cells with increased chondrogenic potential for regenerative medicine. Stem Cells Transl Med 2016;6:77–87.
[12] Skalska U, Kontny E. Adipose-derived mesenchymal stem cells from infrapatellar fat pad of patients with rheumatoid arthritis and osteoarthritis have comparable immunomodulatory properties. Autoimmunity 2016;49:124–31.
[13] Garcia J, Wright K, Roberts S, Kuiper JH, Mangham C, Richardson J, et al. Characterisation of synovial fluid and infrapatellar fat pad derived mesenchymal stromal cells: the influence of tissue source and inflammatory stimulus. Sci Rep 2016;6:24295.
[14] do Amaral RJFC, Almeida HV, Kelly DJ, O'Brien FJ, Kearney CJ. Infrapatellar fat pad stem cells: from developmental biology to cell therapy. Stem Cells International 2017;2017. 6843727–10.
[15] Dragoo JL, Samimi B, Zhu M, Hame SL, Thomas BJ, Lieberman JR, et al. Tissue-engineered cartilage and bone using stem cells from human infrapatellar fat pads. J Bone Joint Surg Br 2003;85:740–7.
[16] Ding D-C, Wu K-C, Chou H-L, Hung W-T, Liu H-W, Chu T-Y. Human infrapatellar fat pad-derived stromal cells have more potent differentiation capacity than other mesenchymal cells and can be enhanced by hyaluronan. Cell Transplant 2015;24:1221–32.
[17] Sun Y, Chen S, Pei M. Comparative advantages of infrapatellar fat pad: an emerging stem cell source for regenerative medicine. Rheumatology (Oxford) 2018;57:2072–86.
[18] Kouroupis D, Bowles AC, Willman MA, Perucca Orfei C, Colombini A, Best TM, et al. Infrapatellar fat pad-derived MSC response to inflammation and fibrosis induces an immunomodulatory phenotype involving CD10-mediated Substance P degradation. Sci Rep 2019;9:10864.
[19] Bailey AM, Mendicino M, Au P. An FDA perspective on preclinical development of cell-based regenerative medicine products. Nat Biotechnol 2014;32:721–3.
[20] Mendicino M, Bailey AM, Wonnacott K, Puri RK, Bauer SR. MSC-based product characterization for clinical trials: an FDA perspective. Cell Stem Cell 2014;14:141–5.
[21] Friedner OM, Allickson JG, Zhang N, Jung S, Fiorentini D, Abraham E, et al. A consensus introduction to serum replacements and serum-free media for cellular therapies. Cytotherapy 2017;19:155–69.
[22] Stolzing A, Jones E, McGonagle D, Scutt A. Age-related changes in human bone marrow-derived mesenchymal stem cells: consequences for cell therapies. Mech Ageing Dev 2008;129:163–73.
[23] Galipeau J, Sensebé L. Mesenchymal stromal cells: clinical challenges and therapeutic opportunities. Cell Stem Cell 2018;22:824–33.
[24] Doucet C, Ernou I, Zhang Y, Llense J-R, Begot L, Holy X, et al. Platelet lysates promote mesenchymal stem cell expansion: a safety substitute for animal serum in cell-based therapy applications. J Cell Physiol 2005;205:228–36.
[25] Jung S, Sen A, Rosenberg L, Behie LA. Identification of growth and attachment factors for the serum-free isolation and expansion of human mesenchymal stromal cells. Cytotherapy 2010;12:637–57.
[26] Fekete N, Gadelorge M, Fürst D, Maurer C, Dausend J, Fleury-Cappellesso S, et al. Platelet lysate from whole blood-derived pooled platelet concentrates and apheresis-derived platelet concentrates for the isolation and expansion of human

bone marrow mesenchymal stromal cells: production process, content and identification of active components. Cytotherapy 2012;14:540–54.
[27] Griffiths S, Baraniak PR, Copland IB, Nerem RM, McDevitt TC. Human platelet lysate stimulates high-passage and senescent human multipotent mesenchymal stromal cell growth and rejuvenation *in vitro*. Cytotherapy 2013;15:1469–83.
[28] Hemeda H, Giebel B, Wagner W. Evaluation of human platelet lysate versus fetal bovine serum for culture of mesenchymal stromal cells. Cytotherapy 2014;16:170–80.
[29] Trojahn Kølle S-F, Oliveri RS, Glovinski PV, Kirchhoff M, Mathiasen AB, Elberg JJ, et al. Pooled human platelet lysate versus fetal bovine serum—investigating the proliferation rate, chromosome stability and angiogenic potential of human adipose tissue-derived stem cells intended for clinical use. Cytotherapy 2013;15:1086–97.
[30] Altaie A, Baboolal TG, Wall O, Jones E, McGonagle D. Platelet lysate enhances synovial fluid multipotential stromal cells functions: implications for therapeutic use. Cytotherapy 2018;20:375–84.
[31] Søndergaard RH, Follin B, Lund LD, Juhl M, Ekblond A, Kastrup J, et al. Senescence and quiescence in adipose-derived stromal cells: effects of human platelet lysate, fetal bovine serum and hypoxia. Cytotherapy 2017;19:95–106.
[32] Martinelli D, Pereira RC, Mogni M, Benelli R, Mastrogiacomo M, Coviello D, et al. A humanized system to expand *in vitro* amniotic fluid-derived stem cells intended for clinical application. Cytotherapy 2016;18:438–51.
[33] Kong CM, Lin HD, Biswas A, Bongso A, Fong C-Y. Manufacturing of human Wharton's jelly stem cells for clinical use: selection of serum is important. Cytotherapy 2019;21:483–95.
[34] Glovinski PV, Herly M, Mathiasen AB, Svalgaard JD, Borup R, Talman M-LM, et al. Overcoming the bottleneck of platelet lysate supply in large-scale clinical expansion of adipose-derived stem cells: a comparison of fresh versus three types of platelet lysates from outdated buffy coat-derived platelet concentrates. Cytotherapy 2017;19:222–34.
[35] Muraglia A, Todeschi MR, Papait A, Poggi A, Spanò R, Strada P, et al. Combined platelet and plasma derivatives enhance proliferation of stem/progenitor cells maintaining their differentiation potential. Cytotherapy 2015;17:1793–806.
[36] Lucchini G, Introna M, Dander E, Rovelli A, Balduzzi A, Bonanomi S, et al. Platelet-lysate-expanded mesenchymal stromal cells as a salvage therapy for severe resistant graft-versus-host disease in a pediatric population. Biol Blood Marrow Transplant 2010;16:1293–301.
[37] Bonin von M, Stölzel F, Goedecke A, Richter K, Wuschek N, Hölig K, et al. Treatment of refractory acute GVHD with third-party MSC expanded in platelet lysate-containing medium. Bone Marrow Transplant 2009;43:245–51.
[38] Phinney DG, Galipeau J. Msc Committee Of The International Society Of C, Gene T. Manufacturing mesenchymal stromal cells for clinical applications: a survey of Good Manufacturing Practices at U.S. academic centers. Cytotherapy 2019;21:782–92.
[39] Oikonomopoulos A, van Deen WK, Manansala A-R, Lacey PN, Tomakili TA, Ziman A, et al. Optimization of human mesenchymal stem cell manufacturing: the effects of animal/xeno-free media. Sci Rep 2015;5. 16570−11.
[40] Fernandez-Rebollo E, Mentrup B, Ebert R, Franzen J, Abagnale G, Sieben T, et al. Human platelet lysate versus fetal calf serum: these supplements do not select for different mesenchymal stromal cells. Sci Rep 2017;7:5132–8.
[41] Heathman TRJ, Stolzing A, Fabian C, Rafiq QA, Coopman K, Nienow AW, et al. Serum-free process development: improving the yield and consistency of human mesenchymal stromal cell production. Cytotherapy 2015;17:1524–35.
[42] Al-Saqi SH, Saliem M, Asikainen S, Quezada HC, Ekblad A, Hovatta O, et al. Defined serum-free media for *in vitro* expansion of adipose-derived mesenchymal stem cells. Cytotherapy 2014;16:915–26.
[43] Kouroupis D, Bowles AC, Best TM, Kaplan LD, Correa D. CD10/neprilysin enrichment in infrapatellar fat pad-derived mesenchymal stem cells under regulatory-compliant conditions: implications for efficient synovitis and fat pad fibrosis reversal. Am J Sports Med 2020;48:2013–27.
[44] Kouroupis D, Churchman SM, McGonagle D, Jones EA. The assessment of CD146-based cell sorting and telomere length analysis for establishing the identity of mesenchymal stem cells in human umbilical cord. F1000Research 2014;3:126.
[45] Jones E, English A, Churchman SM, Kouroupis D, Boxall SA, Kinsey S, et al. Large-scale extraction and characterization of CD271+ multipotential stromal cells from trabecular bone in health and osteoarthritis: implications for bone regeneration strategies based on uncultured or minimally cultured multipotential stromal cells. Arthritis Rheum 2010;62:1944–54.
[46] Cawthon RM. Telomere measurement by quantitative PCR. Nucleic Acids Res 2002;30. e47−7.
[47] Szklarczyk D, Franceschini A, Wyder S, Forslund K, Heller D, Huerta-Cepas J, et al. STRING v10: protein-protein interaction networks, integrated over the tree of life. Nucleic Acids Res 2015;43:D447–52.
[48] Brun J, Abruzzese T, Rolauffs B, Aicher WK, Hart ML. Choice of xenogenic-free expansion media significantly influences the myogenic differentiation potential of human bone marrow-derived mesenchymal stromal cells. Cytotherapy 2016;18:344–59.
[49] Barajas-Gómez BA, Rosas-Carrasco O, Morales-Rosales SL, Pedraza Vázquez G, González-Puertos VY, Juárez-Cedillo T, et al. Relationship of inflammatory profile of elderly patients serum and senescence-associated secretory phenotype with human breast cancer cells proliferation: role of IL6/IL8 ratio. Cytokine 2017;91:13–29.
[50] Spees JL, Gregory CA, Singh H, Tucker HA, Peister A, Lynch PJ, et al. Internalized antigens must be removed to prepare hypoimmunogenic mesenchymal stem cells for cell and gene therapy. Mol Ther 2004;9:747–56.
[51] Bobis-Wozowicz S, Kmiotek K, Kania K, Karnas E, Labedz-Maslowska A, Sekula M, et al. Diverse impact of xeno-free conditions on biological and regenerative properties of hUC-MSCs and their extracellular vesicles. J Mol Med 2017;95:205–20.
[52] Gerby S, Attebi E, Vlaski M, Ivanovic Z. A new clinical-scale serum-free xeno-free medium efficient in *ex vivo* amplification of mesenchymal stromal cells does not support mesenchymal stem cells. Transfusion 2017;57:433–9.
[53] Burnouf T, Strunk D, Koh MBC, Schallmoser K. Human platelet lysate: replacing fetal bovine serum as a gold standard for human cell propagation? Biomaterials 2016;76:371–87.
[54] Schallmoser K, Henschler R, Gabriel C, Koh MBC, Burnouf T. Production and quality requirements of human platelet lysate: a position statement from the Working Party on Cellular Therapies of the International Society of Blood Transfusion. Trends Biotechnol 2020;38:13–23.
[55] De Bari C, Dell'Accio F, Karystinou A, Guillot PV, Fisk NM, Jones EA, et al. A biomarker-based mathematical model to predict bone-forming potency of human synovial and periosteal mesenchymal stem cells. Arthritis Rheum 2008;58:240–50.
[56] Ong WK, Tan CS, Chan KL, Goesantoso GG, Chan XHD, Chan E, et al. Identification of specific cell-surface markers of adipose-derived stem cells from subcutaneous and visceral fat depots. Stem Cell Reports 2014;2:171–9.
[57] Su X, Zuo W, Wu Z, Chen J, Wu N, Ma P, et al. CD146 as a new marker for an increased chondroprogenitor cell sub-population in the later stages of osteoarthritis. J Orthop Res 2015;33:84–91.
[58] Wu C-C, Liu F-L, Sytwu H-K, Tsai C-Y, Chang D-M. CD146+ mesenchymal stem cells display greater therapeutic potential than CD146− cells for treating collagen-induced arthritis in mice. Stem Cell Res Ther 2016;7:23.
[59] Bardin N, Blot-Chabaud M, Despoix N, Kebir A, Harhouri K, Arsanto J-P, et al. CD146 and its soluble form regulate monocyte transendothelial migration. Arterioscler Thromb Vasc Biol 2009;29:746–53.
[60] Ma S, Xie N, Li W, Yuan B, Shi Y, Wang Y. Immunobiology of mesenchymal stem cells. Cell Death Differ 2014;21:216–25.
[61] Addison CL, Daniel TO, Burdick MD, Liu H, Ehlert JE, Xue YY, et al. The CXC chemokine receptor 2, CXCR2, is the putative receptor for ELR+ CXC chemokine-induced angiogenic activity. J Immunol 2000;165:5269–77.
[62] Shapouri-Moghaddam A, Mohammadian S, Vazini H, Taghadosi M, Esmaeili S-A, Mardani F, et al. Macrophage plasticity, polarization, and function in health and disease. J Cell Physiol 2018;233:6425–40.
[63] Ip WKE, Hoshi N, Shouval DS, Snapper S, Medzhitov R. Anti-inflammatory effect of IL-10 mediated by metabolic reprogramming of macrophages. Science 2017;356:513–9.
[64] Chen L, Zhang Q, Chen Q-H, Ran F-Y, Yu L-M, Liu X, et al. Combination of G-CSF and AMD3100 improves the anti-inflammatory effect of mesenchymal stem cells on inducing M2 polarization of macrophages through NF-κB-IL1RA signaling pathway. Front Pharmacol 2019;10:579.
[65] Kim H-K, Lee S-G, Lee S-W, Oh BJ, Kim JH, Kim J-A, et al. A subset of paracrine factors as efficient biomarkers for predicting vascular regenerative efficacy of mesenchymal stromal/stem cells. Stem Cells 2019;37:77–88.
[66] Brizzi MF, Battaglia E, Montrucchio G, Dentelli P, Del Sorbo L, Garbarino G, et al. Thrombopoietin stimulates endothelial cell motility and neoangiogenesis by a platelet-activating factor-dependent mechanism. Circ Res 1999;84:785–96.
[67] Park HY, Kwon HM, Lim HJ, Hong BK, Lee JY, Park BE, et al. Potential role of leptin in angiogenesis: leptin induces endothelial cell proliferation and expression of matrix metalloproteinases *in vivo* and *in vitro*. Exp Mol Med 2001;33:95–102.
[68] Katzman SD, Hoyer KK, Dooms H, Gratz IK, Rosenblum MD, Paw JS, et al. Opposing functions of IL-2 and IL-7 in the regulation of immune responses. Cytokine 2011;56:116–21.
[69] Tabernero J. The role of VEGF and EGFR inhibition: implications for combining anti-VEGF and anti-EGFR agents. Mol Cancer Res 2007;5:203–20.
[70] Battegay EJ, Rupp J, Iruela-Arispe L, Sage EH, Pech M. PDGF-BB modulates endothelial proliferation and angiogenesis *in vitro* via PDGF beta-receptors. J Cell Biol 1994;125:917–28.
[71] Brew K, Nagase H. The tissue inhibitors of metalloproteinases (TIMPs): an ancient family with structural and functional diversity. Biochim Biophys Acta 2010;1803:55–71.
[72] Waterman RS, Tomchuck SL, Henkle SL, Betancourt AM. A new mesenchymal stem cell (MSC) paradigm: polarization into a pro-inflammatory MSC1 or an immunosuppressive MSC2 phenotype. PLoS One 2010;5:e10088.
[73] Bernardo ME, Fibbe WE. Mesenchymal stromal cells: sensors and switchers of inflammation. Cell Stem Cell2013;13:392−402.
[74] François M, Romieu-Mourez R, Li M, Galipeau J. Human MSC suppression correlates with cytokine induction of indoleamine 2,3-dioxygenase and bystander M2 macrophage differentiation. Mol Ther 2012;20:187–95.
[75] Melief SM, Geutskens SB, Fibbe WE, Roelofs H. Multipotent stromal cells skew monocytes towards an anti-inflammatory interleukin-10-producing phenotype by production of interleukin-6. Haematologica 2013;98:888−95.
[76] Németh K, Leelahavanichkul A, Yuen PST, Mayer B, Parmelee A, Doi K, et al. Bone marrow stromal cells attenuate sepsis via prostaglandin E(2)-dependent reprogramming of host macrophages to increase their interleukin-10 production. Nat Med 2009;15:42–9.
[77] Najar M, Raicevic G, Boufker HI, Fayyad Kazan H, De Bruyn C, Meuleman N, et al. Mesenchymal stromal cells use PGE2 to modulate activation and proliferation of lymphocyte subsets: combined comparison of adipose tissue, Wharton's jelly and bone marrow sources. Cell Immunol 2010;264:171–9.
[78] Ren G, Su J, Zhang L, Zhao X, Ling W, L'huillie A, et al. Species variation in the mechanisms of mesenchymal stem cell-mediated immunosuppression. Stem Cells 2009;27:1954–62.
[79] Duffy MM, Pindjakova J, Hanley SA, McCarthy C, Weidhofer GA, Sweeney EM, et al. Mesenchymal stem cell inhibition of T-helper 17 cell- differentiation is triggered by cell-cell contact and mediated by prostaglandin E2 via the EP4 receptor. Eur J Immunol 2011;41:2840–51.